HHS Public Access

Author manuscript

Mater Sci Eng C Mater Biol Appl. Author manuscript; available in PMC 2018 March 01.

Published in final edited form as:

Mater Sci Eng C Mater Biol Appl. 2017 March 01; 72: 238–251. doi:10.1016/j.msec.2016.11.029.

Evaluation of Poly(Lactic-co-Glycolic Acid) and Poly(DL-Lactide-co-ε-Caprolactone) Electrospun Fibers for the Treatment of HSV-2 Infection

Stella E. Aniagyei[1,**], **Lee B. Sims**[1,**], **Danial A. Malik**[3,**], **Kevin M. Tyo**[3,5,**], **Keegan C. Curry**[1,**], **Woihwan Kim**[2,**], **Daniel A. Hodge**[1,**], **Jinghua Duan**[1,5,**], and **Jill M. Steinbach-Rankins**[1,3,4,5,*]

[1]Department of Bioengineering, University of Louisville, Louisville, KY 40202

[2]Department of Medicine, University of Louisville, Louisville, KY 40202

[3]Department of Pharmacology and Toxicology, University of Louisville, Louisville, KY 40202

[4]Department of Microbiology and Immunology, University of Louisville, Louisville, KY 40202

[5]Center for Predictive Medicine, University of Louisville, Louisville, KY 40202

Abstract

More diverse multipurpose prevention technologies are urgently needed to provide localized, topical pre-exposure prophylaxis against sexually transmitted infections (STIs). In this work, we established the foundation for a multipurpose platform, in the form of polymeric electrospun fibers (EFs), to physicochemically treat herpes simplex virus 2 (HSV-2) infection. To initiate this study, we fabricated different formulations of poly(lactic-co-glycolic acid) (PLGA) and poly(DL-lactide-co-ε-caprolactone) (PLCL) EFs that encapsulate Acyclovir (ACV), to treat HSV-2 infection *in vitro*. Our goals were to assess the release and efficacy differences provided by these two different biodegradable polymers, and to determine how differing concentrations of ACV affected fiber efficacy against HSV-2 infection and the safety of each platform *in vitro*. Each formulation of PLGA and PLCL EFs exhibited high encapsulation efficiency of ACV, sustained-delivery of ACV through one month, and *in vitro* biocompatibility at the highest doses of EFs tested. Additionally, all EF formulations provided complete and efficacious protection against HSV-2 infection *in vitro*, regardless of the timeframe of collected fiber eluates tested. This work demonstrates the potential for PLGA and PLCL EFs as delivery platforms against HSV-2, and indicates that these delivery vehicles may be expanded upon to provide protection against other sexually transmitted infections.

*Corresponding author: University of Louisville, 505 S. Hancock St., CTRB, Room 623, Louisville, KY 40202, Phone: (502) 852-5486, Fax: (502) 852-5468, jill.steinbach@louisville.edu.

**Contributed equally

Keywords

Electrospun Fibers; Herpes Simplex Virus 2 (HSV-2); Sexually Transmitted Infections (STIs); Microbicide; Antiviral; Acyclovir; Intravaginal; Drug Delivery Systems

1. Introduction

A multipurpose, safe, and effective microbicide has the potential to prevent millions of sexually transmitted infections (STIs) globally. While STIs as a whole affect approximately 340 million new people each year, herpes simplex virus 2 (HSV-2) is particularly pervasive, affecting 536 million people worldwide, and causing an estimated 23 million new infections each year [1–6]. Furthermore, infection with HSV-2 increases the propensity of co-infection with other STIs, such as human immunodeficiency virus (HIV) by 2 to 6-fold [7–12]. Yet, despite the crucial need to develop prophylactic agents and therapeutics, vaccines and oral antivirals have only been moderately successful in preventing STIs and curing them post-infection. Microbicides, in comparison, have the potential to offer a promising alternative to prevent and treat STIs, while imparting female-controlled protection against a diversity of infections.

Next-generation microbicides seek to incorporate multipurpose prevention technologies that can prevent and treat a diversity of STIs, including HSV-2 and HIV, while also providing prolonged release, specificity, simultaneous delivery of antivirals with biologics, and safety and durability in the female reproductive tract. While recent clinical trials have demonstrated that frequent application of oral anti(retro)virals or topical vaginal microbicides can reduce STI transmission, these trials have underscored the need for new approaches to improve long-term efficacy and user adherence [13–28]. Yet, despite their potential, the scarcity of multipurpose technologies that offer long-term (> 1 month) administration to the unique microenvironment of the female reproductive tract has hindered microbicide success.

Thus far, many of the microbicide delivery vehicles in preclinical or clinical trials consist of gels and intravaginal rings (IVRs) [19, 20, 23, 29–35]. Vaginal gels may be prone to user adherence challenges, due to their viscous “leaky” formulations, relative to more solid delivery platforms such as IVRs. Due to the discomfort associated with vaginal leakage, gels have been shown to be less acceptable among users [22, 36–43]. While IVRs by comparison offer a more discreet option to provide prolonged protection, until recently, IVRs were challenged with providing the release of both hydrophilic and hydrophobic molecules from one delivery vehicle [27, 44–49]. Moreover, the high temperature processing conditions often associated with IVR fabrication may prove challenging for the incorporation of biological agents. These challenges in combination with the need to increase user adherence, highlight the need for new microbicide delivery platforms. To address these needs, electrospun fibers (EFs) have emerged as a delivery platform to offer early- and sustained-delivery of antiviral agents to the female reproductive tract [50–56].

While EFs have been successfully used in many other delivery applications [57–59]; EFs have only recently been explored for microbicide delivery [35, 50, 52–54, 56, 60–62]. Due to their ability to incorporate a diversity of agents with different temporal release

characteristics, EFs have the potential to provide prolonged delivery systems for topical active agent delivery to the female reproductive tract. To demonstrate tunable delivery, to date, EF formulations have primarily focused on HIV prevention. Ball et al. developed poly(L-lactic acid)/polyethylene oxide (PLLA/PEO) and polyvinylpyrrolidone (PVP) or PEO fibers for the delivery of anti-HIV and contraceptive agents [53, 55]; whereas Blakney et al. assessed different multiscale geometries for delivery candidates for HIV prevention and unintended pregnancy [56], and Krogstad et al. evaluated the potential to scale-up manufacturing of polyvinyl alcohol (PVA) fibers [51]. Most recently poly(lactic-co-glycolic acid) (PLGA) and polycaprolactone (PCL) fiber blends were investigated for the delivery of Tenofovir against HIV infection [61]. To exemplify stimuli-responsive tunability, Huang et al. have taken a different approach to evaluate cellulose acetate phthalate fibers for semen-induced release of TDF [50] and have utilized polystyrene fibers to entrap HIV [54]. While many of these EF platforms have focused on HIV inhibition, their effect on HSV-2 inhibition has been less thoroughly explored.

In our previous work, we developed a safe and effective microbicide, using poly(lactic-co-glycolic acid) (PLGA) nanoparticles that encapsulate siRNA targeting host receptors, to significantly increase survival in a murine model after a lethal dose of HSV-2 infection [63]. Our goal here was to expand our materials expertise into electrospun fibers, utilizing similar biodegradable polymers that might complement nanoparticle delivery, as a more durable platform to remain in and prolong delivery to the female reproductive tract. Building the foundation for this platform, our aim was to utilize our expertise in biodegradable polymers and HSV-2 infection, to develop and compare the feasibility of two FDA-approved biodegradable polymers, PLGA and poly(DL-lactide-co-ε-caprolactone) (PLCL), electrospun into fibers, to provide early- and sustained-delivery of a model HSV-2 antiviral, ACV.

We selected PLGA and PLCL, as model polymers, as they are known for their biocompatibility across a variety of applications in different vehicular forms and long-term durability in *in vivo* applications including stents and tissue engineering [64–68]. Furthermore, both PLGA and PLCL have outstanding sustained-delivery properties, demonstrating release in both microbicide and other delivery applications from months to years [35, 61, 64, 68–70]. PLGA can be copolymerized to optimize both the mechanical fiber properties and release profiles of encapsulated materials, while PLCL has demonstrated more favorable intermediate release compared to the rapid degradation of poly(lactic acid) (PLA) or prolonged release of PCL [71]. Due to these attributes and similar biocompatibility [72], we selected these platforms for comparison of ACV incorporation and fiber functionality.

Our goal in this work was to develop, test, and compare two different biodegradable EF platforms that address the needs of short- and long-term microbicide delivery by: achieving early short-term release accompanied by prolonged sustained-release; ensuring high encapsulant loading; exhibiting biocompatibility; and providing complete *in vitro* efficacy against HSV-2 infection. We were specifically interested in characterizing the release profiles from these fibers, establishing their functionality against HSV-2 infection, and determining their safety *in vitro*. Here we demonstrate that PLGA and PLCL EFs highly

encapsulate and provide early burst- and long-term sustained-release of ACV for up to one month. We determined that all formulation eluates completely inhibited HSV-2 infection after a variety of release times *in vitro*. Additionally, as a secondary mode of barrier protection, both PLGA and PLCL EFs physically decreased virus penetration *in vitro* for up to 72 hr. To our knowledge this is the first study to compare the feasibility of two different biodegradable electrospun fiber platforms PLGA and PLCL EFs to offer early- and sustained-delivery of ACV, and subsequent physicochemical protection against HSV-2 transmission *in vitro*.

2. Materials and methods

2.1. Materials

Poly(DL-lactide-co-ε-caprolactone) 80:20 (PLCL, 0.75 dL/g, 37 kDa MW), obtained from Lakeshore Biomaterials (Birmingham, AL), was kindly provided by Dr. Stuart Williams III. Carboxylic acid terminated 50:50 poly(DL-lactide-co-glycolide) (PLGA, 0.55–0.75 dL/g, 31–57 kDa MW) was purchased from Lactel Absorbable Polymers (Cupertino, CA). Acyclovir (ACV), polyvinyl alcohol (PVA), dichloromethane (DCM), chloroform (CF), N,N-dimethylformamide (DMF), and dimethyl sulfoxide (DMSO) were obtained from Sigma Aldrich (St Louis, MO). 1,1,1,3,3,3—hexafluoro-2-propanol (HFIP) and trifluoroethanol (TFE) were obtained from Fisher Scientific (Pittsburgh, PA). African green monkey kidney (Vero E6) cells, human cervical carcinoma (HeLa) cells, and HSV-2 (4674) were kindly provided by Dr. Kenneth Palmer (University of Louisville). Fetal bovine serum (FBS), antibiotics (penicillin/streptomycin) and Minimum Essential Medium (MEM) were purchased from VWR. Simulated vaginal fluid (SVF) was prepared as described in [73].

2.2. Synthesis of Electrospun Fibers

PLGA and PLCL EFs were prepared and electrospun with different solvents and compositions spanning (8–30% wt drug/wt polymer (w/w)) to establish a baseline blank EF (no drug) formulation. For blank polymer EFs, solutions of 10–30% PLGA w/w and 8–12% PLCL w/w were prepared in various solvents (CF:DMF (3:1 and 9:1 vol%), TFE, or HFIP) and allowed to solubilize overnight on a shaker at room temperature. Three milliliters of each polymer solution were aspirated into, and spun from a 3 mL plastic syringe on a custom built device housed in an air-filtered Plexiglas chamber. Flow rates spanning (0.5 – 3.0 mL/hr) were optimized over a range of voltages (15–27 kV) and the resulting fiber mat was collected on a rotating 4 or 26 mm outer diameter stainless steel mandrel, located 25 cm from the blunt needle tip. Sample flow rate was monitored by an infusion pump (Fisher Scientific, Pittsburgh, PA) and the voltage was applied using a high voltage power supply (Spellman CZE 1000R). Final optimized formulations of fibers were spun at 27 kV at 2.0 mL/hr for both PLGA and PLCL formulations. For ACV incorporation, fibers were prepared with 1, 10, and 20% w/w ACV (to polymer) dissolved in polymer solution overnight. After electrospinning, fibers were removed from the mandrel and dried overnight in a desiccator cabinet.

2.3 Electrospun Fiber Solution Conductivity and Viscometry

The impact of solvent choice, polymer composition and ACV concentration on conductivity and viscosity were assessed. To assess conductivity, solvent alone (HFIP, TFE, 3:1 CF:DMF, or 9:1 CF:DMF); solvent plus polymer (HFIP plus 15% PLGA or 12% PLCL); or HFIP plus PLGA or PLCL and 20% ACV were prepared in 3mL aliquots the night before testing. Conductivity measurements were performed using a NanoBrook ZetaPALS zeta-potential analyzer (Brookhaven Instruments), courtesy of Dr. Martin O'Toole (University of Louisville). Solvent solutions were pipetted into fresh cuvettes, followed by submerging the conductivity probe into solution. Prior to sample measurements, deionized water and a known conductivity standard (1000 μS/cm) were assessed to ensure instrument functionality.

To measure the viscosity of the polymer solutions and selected solvents, polymer-solvent samples were prepared the day prior to testing. For the initial formulations, solvents (HFIP, TFE, 3:1 CF:DMF, or 9:1 CF:DMF) plus PLGA were measured to assess spinnability for a given formulation. Due to the favorable viscosity and corresponding fibers obtained with HFIP, we next examined the change in fiber (PLGA and PLCL) solution viscosities after addition of 1, 10, or 20% ACV. Solutions were manually pipetted into the modular compact rheometer (Physica MCR 300, Anton Paar) for measurement. Solvent alone and blank polymer solutions were assessed to verify instrument accuracy.

2.4. Electrospun Fiber Size and Morphology

The impact of solvent choice, polymer composition, and ACV concentration on fiber morphology and size were evaluated using scanning electron microscopy (SEM). After desiccation, EFs were placed on carbon tape, sputter coated with gold, and imaged using SEM (JSM-820, JEOL, Tokyo, Japan). SEM images were acquired at the appropriate magnifications to enable clear visualization of the fiber microstructure. All EF diameters were obtained by analyzing SEM images with NIH ImageJ. To determine the mean and median EF diameters of each formulation, line elements were drawn across a minimum of 50 fibers per image. Statistical significance of fiber diameter was assessed using a student's t-test, with statistical significance determined for $p < 0.05$.

In addition to fiber diameter, SEM was used to measure the average pore sizes for blank PLGA and PLCL fibers. The SEM images were converted to binary images using a threshold to only visualize the top layer of fibers. Relative open area (ROA) was then calculated by computing the area fraction of background to nanofiber material. Fiber porosity and ROA have been found to be equivalent in randomly organized structures [74]. Based on the inherent randomness of fiber alignment, this assumption was applied to our porosity assessment.

2.5. Fiber Characterization: Loading, Encapsulation Efficiency, and Controlled Release

The amount of ACV incorporated within the fibers was quantified by dissolving 3–5 mg EFs in 500 μL DCM for 30 min. Subsequently, 500 μL Tris-EDTA (TE) buffer was added to the DCM-fiber solution, and vortexed for one minute. Samples were immediately centrifuged at 4°C at 12,500 rpm for 10 min to extract the aqueous supernatant. After the first centrifuge, the TE supernatant was removed and placed in a collection tube. An equal volume of TE

was again added to the DCM extraction solution, vortexed for one minute, centrifuged as above, and extracted. The loading of ACV, defined as the amount of ACV incorporated per milligram of fiber, was measured from the extracted supernatant using UV absorption spectroscopy at 254 nm. Encapsulation efficiency, or the percent ACV incorporated relative to the amount of ACV initially loaded, was calculated as follows: [(Mass of ACV incorporated per mg of EF) / (Mass of ACV initially added to electrospinning solution per mg of EF)] x 100.

To determine the sustained-release profiles of the EFs *in vitro*, triplicate fiber pieces of 5–10 mg were cut and suspended in 2–10 mL of SVF in 15 mL conical polypropylene tubes. SVF was used to mimic similar conditions within the female reproductive tract. EF samples were incubated at 37°C and constantly shaken. At each of the following time points: 1, 2, 4, 6, 24, 48, 72, 168 (1 week), 336 (2 weeks), 504 (3 weeks), and 672 hr (4 weeks), the complete volume of SVF was removed and replaced with fresh SVF. All samples were analyzed in triplicate.

2.6. Fiber Morphology, Degradation, and Mechanical Testing

To evaluate EF degradation *in vitro*, 10 mg PLGA or PLCL EFs were immersed in 1 mL SVF at 37°C for up to one month. Both mass loss and the change in fiber morphology were evaluated as a function of time. Samples were removed at: 0, 3, 7, 14, 21, and 28 days to assess fiber morphology via SEM, and to determine the percent mass loss of each sample.

Additionally, for blank PLGA and PLCL fibers, mechanical testing of the electrospun fibers was performed by trimming the electrospun fibers into “bone”-shaped sheets (Supplementary Figure 1). The sample width and thickness were recorded in the middle, where the thickness was taken as the average of the three points and the width was taken at the thinnest point, to determine the fiber stress. For PLGA, the width and thickness varied from 7.67 to 11.09 mm and 0.15 mm to 0.19 mm, respectively; whereas for PLCL the width and thickness spanned 14.07 to 16.36 mm and 0.08 mm to 0.10 mm, respectively. The fiber samples were then loaded in the tensile testing machine (Shimadzu Model EZ-test-500N REV. C #620688–04) kindly provided by Dr. Thomas Berfield (University of Louisville), by placing the top or the bottom of the sample between two pieces of thin plastic and clamping the fiber such that the center of the fiber matched horizontally with the center line indicated on the clamp. The mechanical tests were conducted with the WinAGSLite 2000 program. The starting length was recorded in millimeters by measuring the distance between the two clamps, ranging from 21.26 to 26.92 mm for PLGA and from 19.04 to 24.55 mm for PLCL. The test speed and maximum force were set to 5 mm/min and 100 N. The test was begun to assess Load/Stress and Extension measurements. When the fiber snapped (resulting in the “Load/Stress” value dropping to 0), the test ended. After the data was collected, the cross-sectional area was calculated by multiplying the fiber width by the depth. The stress was calculated by dividing the “Load” by the cross-sectional area. The strain was calculated by dividing the “Position” by the starting value (GL). A stress vs. strain scatter plot graph was created and the line-of-best-fit was calculated. Both the slope (the Young’s Modulus value) and its R^2 value were recorded. The tensile strength was calculated by finding the maximum stress value and the toughness was calculated by entering in the function “=(([$Stress_n$]+

[$Stress_{n+1}$])/2)([$Strain_{n+1}$−$Strain_n$])" and applying it to all positive stress values of n. The sum of the areas was then calculated with the function "=SUM([Area column])" and was recorded as the toughness value. Using this methodology, the sum and sample standard deviation of tensile strength, toughness, and the Young's modulus were calculated for each fiber type. Measurements were calculated as an average of three samples, with associated standard deviation.

2.7. In Vitro Efficacy of PLGA and PLCL EFs against HSV-2 Infection

Eluate Collection to Assess Efficacy at Different Fiber Release Time Points— Viral plaque assays were conducted to test the *in vitro* efficacy of ACV EFs against HSV-2 infection. To assess the differences in ACV fiber activity as a function of the duration of ACV release from the fibers, we evaluated the efficacy of fibers (10 mg) that had been maintained in 10 mL SVF for 3 days, 28 days, or only during the last week of release (21–28 days). For the 3 and 28 day samples, 10 mg PLGA and PLCL EFs were incubated in 10 mL SVF for 3 or 28 days, and the release eluate after that time was collected and administered in plaque assays as described below. For the 21–28 day samples, 10 mg PLGA and PLCL EFs were incubated in 10 mL SVF for 21 days, after which time the SVF eluate was removed. The fibers were then re-incubated in fresh SVF to assess the release of ACV during only the fourth week of release (21 to 28 days). On day 28, this eluate (from 21 to 28 days) was removed and used for *in vitro* plaque assay experiments.

Plaque Assay with EF Eluate—The antiviral activity of the ACV released from EFs at the above time points was determined by conducting HSV-2(4674) plaque assays in Vero E6 cells. Vero E6 cells were maintained in MEM, supplemented with 10% FBS, and 1% penicillin streptomycin. Cells were seeded at 600,000 cells per well and grown to near confluence for 24 hr in a 6-well flat bottom plate. Cells were then infected with 500 μL HSV-2 at 1000 PFU/well and incubated for 1 hr at 37°C to allow for virus infection. After one hour, HSV-2 inoculum was removed and replaced with 2 mL of blank or ACV fiber eluate (from 1%, 10%, or 20% ACV PLGA or PLCL EFs) serial dilutions spanning 0.004 μg/mL to 10 μg/mL ACV from the 3 day, 28 day, or 21–28 day controlled release time points. HSV-2 infected cells were incubated with serial dilutions of free ACV to serve as positive controls of HSV-2 inhibition, in parallel with untreated/uninfected cells. Untreated/infected cells were used as a negative control of virus inhibition. Forty-eight hours post-treatment, Vero cells were fixed with methanol for 10 min, stained with 0.1% crystal violet for 30 min, and washed with DI water. Viral plaques were counted, and data were normalized relative to the number of plaques in untreated/infected cells. Samples were analyzed in triplicate and statistical analysis was done in GraphPad Prism 6.0 (GraphPad Prism Software, Inc., San Diego, CA, USA). The 50% maximal inhibitory concentration (IC50) of the free ACV, 20% PLGA ACV and 20% PLCL ACV EFs against HSV-2 was determined by fitting the four-parameter dose-response sigmoidal curve to the data in GraphPad 6.0. Unpaired student t-tests were used to compare the IC50s of the fiber eluates and free ACV formulations at each time point. Results are expressed as the mean ± confidence intervals (C.I.s), deemed statistically significantly different for $p < 0.05$.

2.8. Physical Inhibition of HSV-2 Penetration

The results from other experiments in our lab have indicated that blank PLGA and PLCL EFs (without ACV), may partially inhibit infection after early virus exposure times of 24 and 48 hr. To assess how the physical presence of blank EFs might serve as a potential barrier to HSV-2 penetration to underlying cells, we incubated HSV-2 atop blank fibers for up to 72 hr. Ten milligrams of blank PLGA EFs, blank PLCL EFs, or no EFs were cut in a disk-like shape and inserted in place of membranes removed from Transwell inserts (Corning® Costar®, Fisher Scientific). Inserts containing these blank PLGA, blank PLCL, or no fiber controls were placed in 12-well plates with Vero E6 cells grown to confluence in the plate below (600,000 cells/well). Infectious HSV-2 (1000 PFU/well) was applied to the apical side of the fiber within the transwell inserts, while the fiber bottom maintained contact with underlying cell culture media (Figure 7A). After time points including: 1, 4, 8, 24, 48, or 72 hr, transwell inserts containing the fibers were removed from the wells, and cell media was replaced with 1 mL of new complete plating media with added IgG. After each of the above time points of transwell fiber removal, cells were incubated for an additional 48 hr to allow virus transmission, after which the total number of plaques per well were counted. Viral plaque counts per well, were normalized to the number of plaques per well in untreated/infected cells.

2.9. In Vitro Cytotoxicity of PLGA and PLCL Fibers

To determine the cytotoxic effect of the PLGA and PLCL EFs, HeLa cells were plated at a density of 300,000 cells per well in a 12-well plate. Cells were incubated in triplicate with 1 mg fiber pieces placed in the transwell inserts (1 mg/mL final concentration). No treatment (media alone) and 10% DMSO were used as positive and negative controls of cell viability, respectively. After 1, 3, and 5 days incubation, 10 μL of MTT reagent was added to the cells, cells were lysed, and absorbance was read at 570 nm the following day. The absorbance values of PLGA- and PLCL-treated cells were normalized to untreated cells to obtain percent viability.

3. Results and discussion

3.1. Electrospun Fiber Size and Morphology

Using the electrospinning apparatus shown in Figure 1A, we evaluated the effect of different solvents and co-solvent mixtures on EF morphology, to find the optimal solvent that obtained reproducibly sized and well-formed EFs (Figure 1B). The resulting EFs produced using: HFIP, 3:1 CF:DMF, 9:1 CF:DMF, and TFE solvents are shown in Figure 2A–D. We found that using HFIP most consistently formed well-delineated PLGA fibers (Figure 2A), followed by 3:1 and 9:1 CF:DMF co-solvents (Figure 2B–C); whereas under the conditions we tested, TFE produced fibers with apparent beading on the fiber surface (Figure 2D). The average fiber diameters of the well-delineated EFs made with: HFIP, 3:1 CF:DMF, and 9:1 CF:DMF fiber formulations were 1.7 ± 0.64 μm, 0.75 ± 0.42 μm, and 2.65 ± 1.45 μm, respectively; whereas the beaded TFE fibers had overall smaller fiber diameters when fibers were formed (0.36 ± 0.26 μm). Importantly, HFIP PLGA fibers demonstrated the least adhesivity to the mandrel, maintained the most structural integrity upon removal from the mandrel (Figures 1B and 2E), and demonstrated greater reproducibility relative to using the

other solvents. Therefore HFIP was used in all subsequent experiments to produce PLGA and PLCL ACV fibers.

Both PLGA and PLCL EF morphologies and macroscale structures obtained using HFIP are compared in Figure 2E–F. Both PLGA and PLCL formed well delineated EF microstructures at 15% and 12% w/w, respectively. The differences in the diameters of PLGA and PLCL fibers as a function of ACV content (1, 10, or 20% w/w) are depicted in Figure 2F. Corresponding SEM images for the 1, 10, and 20% PLGA and PLCL fibers are shown in Supplementary Figure 2. Blank PLGA and PLCL EFs had average diameters of 1.70 +/− 0.64 μm and 2.30 +/− 0.38 μm, respectively. The diameters of both PLGA and PLCL fibers decreased as a function of ACV loading, with PLGA EFs having the smallest diameters overall. Fiber diameters were: 0.78 +/− 0.34 μm, 0.54 +/− 0.15 μm; 0.580 +/− 0.19 μm for 1, 10, and 20% ACV PLGA EFs and 1.88 +/− 0.47 μm; 1.23 +/− 0.25 μm; 0.83 +/− 0.17 μm for 1, 10, and 20% ACV PLCL EFs, respectively. Statistically significant differences in fiber diameter as a function of ACV loading, were observed between all fiber formulations except the 10% and 20% ACV PLGA EFs ($p < 0.05$). Additionally, Supplementary Figures 3 and 4 include the histograms of fiber diameter distribution as a function of PLGA/PLCL and ACV content, in addition to the mean and median diameters for each sample (Supplementary Table 1). The correlation factors between fiber diameter and 1, 10, and 20% PLGA and PLCL EFs were determined to be −0.67 and −0.96, respectively, validating the strong inverse correlation between ACV content and fiber diameter for both PLGA and PLCL EFs

Similarly, SEM images were used to assess the average pore size for blank PLGA and PLCL fibers. The average pore sizes of PLGA and PLCL fibers, from a minimum of 50 measurements, were calculated as 9.0 ± 3.7 μm and 11.8 ± 6.7 μm, respectively. Based on the ROA, the PLGA and PLCL fibers were found to have a porosity of 75% and 48%, respectively. Additionally, using the thickness measurements of 150 and 80 μm for PLGA and PLCL fibers, we calculated each fiber to be comprised of a maximum of 88 and 35 fiber layers, respectively (assuming adjacent fibers in the vertical direction).

3.2 Electrospun Fiber Solution Conductivity and Viscometry

All tested polymer solutions and solvents demonstrated conductivity values that were below the instrument's limit of detection (~5 μS/cm, Supplementary Table 2). This is in agreement with cited literature references in which these polymers and solvents were deemed nonconductive, with values listed below the instrument's limit of detection [75–78]. The viscosity of solvent (HFIP, TFE, 3:1 CF:DMF, or 9:1 CF:DMF) plus PLGA, or HFIP solvent (the solvent that produced the most favorable fibers) plus PLGA or PLCL and 1, 10, or 20% ACV are compared in Supplementary Table 3. The viscosity of HFIP plus PLGA (~1307 and 1294 cP) was inherently more viscous than 3:1 CF:DMF, 9:1 CF:DMF, and TFE PLGA mixtures (~90 cP). In addition we observed a decrease in solvent viscosity with the addition of increasing amounts of ACV.

3.3. Fiber Characterization: Loading, Encapsulation Efficiency, and Controlled Release

3.3.1. Loading and Encapsulation Efficiency—To determine the loading and encapsulation efficiency (EE) of ACV in PLGA and PLCL fibers, we evaluated 1, 10, and 20% w/w ACV PLGA and PLCL EFs. Figure 3A shows the amount of ACV incorporated per milligram of fiber. The resulting average loadings for the 1, 10, and 20% fibers were 12.3, 74.9, and 142.8 μg ACV/mg PLGA fiber and 11.5, 71.7, and 157 μg ACV/mg PLCL fiber, respectively. High ACV EEs, defined as the percent of ACV in the electrospinning solution that was incorporated in the fibers, were achieved for all formulations. For PLGA 1, 10, and 20% fibers, 74, 75, and 71% EE was achieved, with similarly high EEs of 82%, 72% and 79% for PLCL EFs, respectively.

3.3.2. Controlled Release and Fiber Degradation—The total cumulative release of ACV from PLGA and PLCL EFs was measured after incubation in SVF over 28 days (Figure 3B). We observed more prominent sustained-release in the 10 and 20% ACV PLGA and PLCL fibers, with increases in release observed with increased incorporation of ACV. Between 21 and 28 days we observed that the PLGA EFs released slightly more ACV than PLCL EFs, for the 20% ACV formulation. After 28 days, 87, 84, and 100% of incorporated ACV was released from the 1, 10, and 20% ACV PLGA and 48, 77, and 83% of incorporated ACV was released from the 1, 10, and 20% ACV PLCL EFs respectively.

3.4 Fiber Morphology, Degradation, and Mechanical Testing

In parallel with controlled release experiments, we evaluated the change in EF morphology and fiber degradation with respect to time, after incubation in SVF (Figure 4A). PLGA and PLCL EFs began to exhibit mass loss of ~2.9 – 8.6% between one and three days incubation; however, mass loss seemed to have negligible effect on EF morphology (Figure 4B). After 7–10 days the mass loss increased to 12.1 and 10.8% for PLGA and PLCL fibers respectively. Between 14 and 21 days, PLGA EF morphology began to appear slightly more melded and mat-like in appearance; whereas PLCL fibers maintained their well-delineated fiber morphology during the one month degradation study. After 28 days, the average mass loss was similarly maintained between PLGA and PLCL fibers, spanning 12–14%. Furthermore, despite the differences in fiber morphology, no statistically significant differences between PLGA and PLCL mass loss were observed.

For mechanical testing prior to degradation, the PLGA and PLCL fibers had average Young's moduli of 34.2 ± 1.9 MPa and 258.8 ± 9.7 MPa. The PLGA and PLCL fibers exhibited mean toughnesses of 3.0 ± 0.8 MPa and 9.9 ± 2.8 MPa, with tensile strengths of 1.8 ± 0.2 MPa and 4.8 ± 1.0 MPa, respectively.

3.5. In Vitro Efficacy of PLGA and PLCL EFs against HSV-2 Infection

To determine the antiviral potential of ACV PLGA and PLCL EFs against HSV-2, we first assessed the efficacy of low (1% ACV), medium (10% ACV), and high dose (20% ACV) PLGA and PLCL fiber eluate collected after 24 hr release from 1 mg/mL fiber in media (a concentration corresponding to the 10 μg/mL ACV in the low 1% ACV EF), against HSV-2 infection *in vitro* (Figure 5). Blank PLGA and PLCL EFs, with no ACV (negative control for virus inhibition) resulted in more than 260 plaques on average, as indicated by the white

dots (Figure 5A and Table 1); whereas 10 μg/mL of free ACV (positive control for virus inhibition) inhibited plaque formation (Figure 5E: left panel and Table 1). Compared to blank fibers, the 1, 10, and 20% ACV PLGA and PLCL fibers completely inhibited infection, as evidenced by negligible plaque formation (Figure 5B–D and Table 1). Infected cells administered no treatment (Figure 5E: right panel and Table 1) served as an additional negative control for virus inhibition with 281 plaques.

While we observed that low (1% ACV), medium (10% ACV), and high (20% ACV) fibers at a concentration of 1 mg/mL demonstrated strong antiviral potential after 1 day *in vitro*, considering the dose estimated for future *in vivo* experiments and potential time frames needed for prolonged protection, we selected the 20% ACV PLGA and PLCL formulations for more thorough evaluation. To assess the longevity of PLGA and PLCL ACV fiber efficacy against HSV-2, we evaluated three durations of fiber release, after: 3, 28, and 21–28 days (as described in the Methods). After each of these durations, fiber eluates were collected, the corresponding ACV concentration in each eluate was measured (in μg/mL), and eluates were diluted for administration to infected cells. Plaque number for each sample was normalized relative to the average plaque number in untreated, infected cells (> 260 plaques). Free ACV was administered as a positive control of virus inhibition to compare the efficacy (IC50) of fiber eluates after 3, 28, or 21–28 days release.

The eluate collected from 20% ACV PLGA and PLCL EFs after 3, 28, or 21–28 day release achieved similar efficacy, relative to free ACV. Here we tested eluate dilutions from each of the collected time point eluates to determine the IC50s for each release eluate. The average IC50s using fiber eluate collected after 3 days were 0.393 μg/mL (C.I. 0.378, 0.408) and 0.226 μg/mL (C.I. 0.215, 0.238) for PLGA and PLCL 20% ACV EFs respectively, compared to an average IC50 of 0.287 μg/mL (C.I. 0.270, 0.305) for free ACV (Figure 6A). Similarly, fibers were assessed after 28 days to ensure bioactivity after one month in SVF (Figure 6B). After 28 days the resulting EF IC50s were 0.426 (C.I. 0.379, 0.459), 0.314 (0.262, 0.375), and 0.293 μg/mL (C.I. 0.275, 0.312) for PLGA EFs, PLCL EFs, and free ACV respectively. Last, we evaluated the effect of eluate released from PLGA and PLCL 20% ACV EFs between 21 and 28 days – during the fourth week of delivery (Figure 6C). Similar IC50s of 0.417 (C.I. 0.388, 0.469) and 0.314 μg/mL (C.I. 0.277, 0.357) were attained for PLGA and PLCL EFs, respectively. For each time point of eluate collection, we evaluated the statistical significance between PLGA 20% ACV and PLCL 20% ACV, against freshly administered free ACV. For the 3 day release eluate, statistical significance was observed between free ACV and PLGA 20% ACV ($p < 0.01$); and between PLGA 20% ACV and PLCL 20% ACV ($p < 0.025$). After 28 days and 21–28 day release, similar statistical significance between IC50s was observed between free ACV and PLGA 20% ($p < 0.005$ and $p < 0.02$) and after 28 days ($p < 0.0015$ and $p < 0.002$). These results demonstrate that PLGA and PLCL ACV EFs maintain similar efficacy to freshly administered free ACV with PLGA resulting in slightly lower efficacy for at least one month after exposure to conditions representative of the female reproductive tract.

3.6. Physical Inhibition of HSV-2 Penetration

To evaluate the potential of blank fibers to provide a physical barrier against HSV-2 infection, we applied HSV-2 to the apical side of PLGA and PLCL EFs and incubated for up to 72 hr with Vero cells. Fibers were evaluated for their ability to prevent HSV-2 from penetrating to underlying Vero cells. During the first 48 hr of EF incubation with HSV-2, we observed that both blank PLGA and PLCL EFs served as a physical barrier to infection. Figure 7A shows the experimental layout with column: (i) no infection, no treatment; (ii) HSV-2 infection, no treatment; (iii) HSV-2 infection, blank PLGA EF treatment; and (iv) HSV-2 infection, blank PLCL EF treatment.

In Figure 7B, representative pictures of plaque penetration assay results are presented for each time point of fiber removal. For all time points, column i (no infection, no treatment) shows no plaques; whereas, column ii (HSV-2 infection, no treatment) shows viral plaque formation after early time points of infection. As infection progresses, plaque number (and corresponding cell death in white) increases, until the virus has been transmitted to all cells, as indicated by empty wells (dead, non-adherent cells washed away during staining). Relative to the no treatment, HSV-2 infection control group (column ii), blank PLGA and PLCL EFs completely inhibited virus penetration and subsequent infection through 48 hr. However, between 48 and 72 hr, virus began to penetrate the fibers and infect underlying cells, with a greater number of infectious plaques observed using PLGA EFs.

3.7. In Vitro Cytotoxicity of PLGA and PLCL Fibers

Last we evaluated the cytotoxicity of PLGA and PLCL EFs on HeLa cells in culture. While no cell toxicity was observed in plaque assays (as evidenced by no cell death and full crystal violet staining), we wanted to evaluate the cytotoxicity of PLGA and PLCL EFs after exposure to a high concentration of 1 mg/mL EFs for 1 to 5 days (Figure 8). Incubation with up to 1 mg/mL of either PLGA or PLCL EFs resulted in minimum cell viabilities of 97%, 93%, and 93% for HeLa cells after 1, 3, and 5 days exposure.

4. Discussion

HSV-2 plays a significant role in facilitating co-infection with other STIs, including HIV, by as much as 6-fold [7–12]. As such, inhibition of HSV-2 infection is expected to have a significant impact on decreasing the likelihood of HIV and other sexually transmitted infections. To better mitigate infection, new sustained-delivery technologies that have the capacity to prevent, treat, and manage multiple STIs simultaneously are urgently needed [3]. To begin to address this need, our goal here was to develop an intravaginal delivery platform comprised of PLGA and PLCL electrospun fibers to deliver and test a proven “model” antiviral, ACV, against HSV-2 infection *in vitro*.

Relative to existing intravaginal drug delivery technologies, such as gels and IVRs, there is a need to develop alternative platforms that are durable and maintained in the female reproductive tract, while also offering sustained-delivery, negligible toxicity, and long-term efficacy. EFs are a promising technology to offer these attributes, while also enabling the encapsulation and delivery of a diversity of agents. Additionally, due to their scaffold-like

properties, electrospun fibers have the potential to offer a physical, in addition to chemical means, of preventing infection [53, 54]. Toward our long-term goal of designing a multipurpose delivery system that extends the applications and longevity of protection in one platform, here we developed and evaluated PLGA and PLCL ACV EFs against HSV-2 infection.

We first demonstrated the ability to fabricate EFs in both sheet and cylindrical shapes (Figure 1) for the future application of administration to the female reproductive tract using two differently sized mandrels (4 and 26 mm). We evaluated a variety of solvents and electrospinning conditions, and found that HFIP produced excellent fiber morphology, suitable fiber texture post-electrospinning, and process reproducibility for both PLGA and PLCL polymer formulations (Figure 2). While HFIP resulted in reproducible, well-delineated fibers, CF:DMF fiber properties were more irreproducible and for TFE specifically, adhesive fibers resulted, that were difficult to detach from the mandrel.

While a number of parameters can be attributed to the reproducible fabrication of well-delineated fiber microstructures, of the parameters tested in our experiments, solvent viscosity as a function of polymer concentration seemed to have the greatest impact on our ability to establish stable versus unstable electrospinning solutions. In our studies, a critical viscosity of PLGA and PLCL (corresponding to 15 and 12% w/w respectively) was needed to attain well-formed fibers with HFIP. Similar critical viscosities (~1300 cP) were determined for both PLGA and PLCL HFIP solutions; whereas polymers spun with TFE or CF:DMF yielded much lower viscosities (~90 cP) for similar weight percent polymer. In addition, both micro- and macroscale visualization and a lack of adhesion to the mandrel, resulted when the PLGA and PLCL polymers were electrospun in HFIP. This is in agreement with other work using PLGA, where PLGA concentration and flow rate, as related to inherent viscosity, is known to significantly impact fiber diameter [79, 80].

In addition to polymer concentration and flow rate, generally more conductive solutions – to a threshold point of conductivity – yield fibers with well-delineated fiber morphologies, in contrast to beaded morphologies [81], as observed with our fibers that were electrospun with TFE. Yet regardless of our processing conditions: varying polymer concentration, flow rate, and electric field, we found it challenging to reproducibly eliminate beads in the TFE formulations. This in combination with our viscosity measurements strongly indicates that a critical polymer concentration and/or solvent viscosity had not been achieved [80, 82, 83]. Additionally, depending on solvent properties, certain solvents can undergo rapid evaporation if the electrospinning jet is unstable, contributing to porous or beaded morphologies. As noted in other electrospinning studies, there is a balance between polymer solubility and maintaining a high enough dielectric constant to form a Taylor cone during electrospinning. Of the solvents tested, HFIP was the most polar solvent, relative to CF:DMF (non-polar:polar aproic), chloroform (non-polar) and TFE (polar protic) [84–86]. Together these factors may have contributed to the enhanced difficulty we observed in obtaining reproducible fibers with solvents other than HFIP. While rapid evaporation in unstable jets can cause irreproducible fibers, conversely, weak solvent volatility or lower evaporation rates can impact the fiber spinning and subsequent structure. Under the conditions we tested, TFE based fibers adhered to the mandrel after electrospinning (Figure

1A), which we attribute here to the lower solvent evaporation rate of TFE, relative to HFIP [87–89]. While EFs have been successfully fabricated using CF:DMF at the given ratios of 3:1 and 9:1 [90, 91], in our hands, fibers produced using these solvents were less reproducible than using HFIP, especially with lower concentrations of PLGA and PLCL (15 and 12% w/w). Therefore we only proceeded to fabricate and test HFIP PLGA and PLCL EFs for ACV incorporation.

While it is well known that solvent viscosity and solution conductivity, among other parameters, can have a significant impact on fiber diameter, the incorporation of active agents in the electrospinning solution often has an effect on fiber diameter. With the incorporation of increased ACV concentrations in the fibers, we observed a decrease in average fiber diameter for both PLGA and PLCL EFs, with all other electrospinning parameters remaining constant. Relative to their blank fiber counterparts, 1, 10, and 20% ACV PLGA and PLCL fibers resulted in fiber diameter decreases of 54, 68, and 66%; and 18, 47, and 64%. In addition, the negative correlation factors of ACV concentration to PLGA/PLCL fiber diameters validated this inverse relationship, with the decrease in fiber diameter more evident for PLCL EFs (−0.96 vs. −0.67) even at low concentrations of ACV incorporation. While no statistically significant differences were observed between blank and 1% ACV EF fiber diameters, the diameters of 10 and 20% ACV PLGA and PLCL EFs significantly decreased as a function of ACV loading. We observed statistically significant differences between all fiber diameters except between the 1% and 10% PLGA, and 1% and 20% PLCL ACV formulations. While we initially attributed this decrease in diameter to the increased conductivity and charge density of the electrospinning solution after addition of ACV, as indicated by our viscosity and conductivity measurements, the viscosity of the electrospinning solution seems to more prominently correlate with fiber diameter (Supplementary Tables 2 and 3). Increased amounts of ACV may have resulted in a less viscous and more unstable electrospinning jet formation, resulting in increased fiber spinning and elongation, leading to a reduction in fiber diameter [92].

Two attributes of utilizing EFs as delivery vehicles, are the encapsulant loading efficiency and the high surface area-to-volume ratio that contribute to both early- and sustained-release. In fact, one of the questions we wanted to answer was how two polymers, both top candidates as drug delivery vehicles would compare in terms of providing sustained-release. For all PLGA and PLCL formulations (1, 10, and 20% ACV), we achieved high loading and encapsulation efficiency ranging from 71 to 82%, with no significant differences observed based on polymer type or percent ACV initially in solution (Figure 3). In combination with high loading, we achieved early release within the first 72 hr, with a corresponding prolonged release over one month, most notably observed for the PLGA EFs (Figure 3). After 21 and 28 days we found that the PLGA formulations released approximately 25% more ACV than PLCL EFs for the 20% ACV formulation, with the 1% and 10% PLGA and PLCL fibers maintaining similar release relative to their respectively loaded PLCL counterpart. Notably, there was a lag in release for the PLGA formulations that we attribute to polymer matrix degradation between 14 and 21 days. Therefore, while the PLCL 1, 10, and 20% ACV EFs may offer greater initial delivery relative to the respective PLGA ACV EFs, for long-term delivery (≥ 21 days), PLGA EFs may provide a better alternative, benefiting from the second phase of release in acidic conditions.

These sustained-release results also correlated with another important factor for long-term delivery the durability of the delivery vehicle defined here by how quickly the polymer loses microstructural conformation or mass during degradation. For both the PLGA and PLCL formulations, we found that degradation was minimal, with an initial mass loss of 8–9% after three days, which corresponds well to the burst release we see within the first 72 hr. During the course of the experiment, there was no statistical difference in mass loss at each time point between formulations, and after 28 days, only 12–14% mass loss resulted for PLCL and PLGA EFs, respectively (Figure 4). Interestingly, between days 14 and 21, PLGA EFs began to demonstrate a more “mat-like” appearance, indicative of individual fibers melding together. In contrast, while losing similar amounts of mass, PLCL EFs maintained their well-delineated structural integrity. This difference is likely attributed to the swelling induced in the PLGA fibers by water uptake, resulting in subsequent fusion of individual fibers. This difference in EF morphology correlates well with increased ACV release from the PLGA formulations between days 14 and 21; whereas, PLCL EF release was less enhanced relative to previous time points. We believe this morphological change of PLGA EF microstructure, coinciding with the additional release from all PLGA formulations around days 14–21, is likely attributed to the second phase of matrix (polymer) degradation typically seen when PLGA is exposed to acidic environments [63]. This suggests that PLGA fibers will prove advantageous in eliciting long-term release in the acidic microenvironment of the female reproductive tract. In addition to swelling and matrix degradation, polymer crystallinity is also a primary factor affecting the degradation of different polymers. For a PLGA co-polymer, polymer chains in the amorphous regions initially degrade via hydrolysis and during this phase little sample mass is lost [79]. Correspondingly, as molecular weight decreases [79], there is an increase in solubility, mass loss, water uptake, and hydrophilicity.

Yet despite this characteristically enhanced matrix degradation and the observed melding of fiber microstructure, PLGA formulations only released slightly more ACV than PLCL. While we initially expected more rapid degradation of a 50:50 PLGA co-polymer, these results are likely dependent on thickness of the fiber scaffold and fiber diameter (surface-to-volume ratio), resulting in variable levels of degradation even for the same co-polymer type. In our studies, considering the durability (low mass loss) of both PLGA and PLCL EFs over 28 days in SVF, we anticipate that either formulation will provide a durable long-term delivery technology, that can be removed if desired, or maintained for longer application periods (such as 28 days) to provide sustained-release to the female reproductive tract.

From a user adherence perspective, an important consideration in moving electrospun fiber technologies forward will be how the degradation and morphology affects user experience. While challenges of leakiness are often associated with intravaginal gel administration, comparatively speaking, we expect that fibers may be confronted with other challenges, namely rigidity or flexibility, which may impact user preference. We envision that an ideal fiber administration regimen might consist of a “leave-in” product, or a product that is removed prior to intercourse (by establishing a high enough tissue concentration to safely do so). While we did not observe fiber particulates during the degradation process, we need to acknowledge that this may result *in vivo*, potentially affecting user experience and prevention.

For mechanical testing prior to degradation, the PLGA and PLCL fibers had average Young's moduli of 34.2 ± 1.9 MPa and 258.8 ± 9.7 MPa. The PLGA and PLCL fibers exhibited mean toughnesses of 3.0 ± 0.8 MPa and 9.9 ± 2.8 MPa, with tensile strengths of 1.8 ± 0.2 MPa and 4.8 ± 1.0 MPa, respectively. These Young's moduli and strength values of the PLGA fibers were within the range seen in other studies, of 41 and 3 MPa [93], respectively for PLGA, and ranging from 25–120 MPa for PCL [53]. As related to degradation, the Young's modulus and strength values for PLGA fibers have been reported between 25–40 MPa and 0.5–1.5 MPa, as it degrades in the human body over 10 weeks. While our initial mechanical measurements correspond well to these reported literature values, it will be important to study how these values relate to actual user preference and comfort. However, with electrospun fibers being a relatively new technology for intravaginal application, both mechanical and user preference factors have yet to be studied in appropriate and non-trivial behavioral studies as part of the future clinical development pipeline. Until such studies can be conducted, these measurements provide a sound baseline for future analysis.

To preliminarily assess the potential of this platform to inhibit HSV-2 transmission, we initially administered the 1, 10, and 20% ACV PLGA and PLCL undiluted 1 day release eluates in a plaque assay (Figure 5). We observed that at the high concentrations (1 mg/mL) we initially tested, that all fibers completely inhibited HSV-2 infection. Based on these results and the fiber formulation we believed would be most applicable to future *in vivo* studies, we thoroughly characterized the 20% PLGA and PLCL ACV EF eluates at different release time points to compare their bioactivity and efficacy with respect to release time. We assessed how the 20% ACV PLGA and PLCL EF eluates at various times: 3, 28, and 21–28 days of release, compared to free ACV in preventing HSV-2 infection (Figure 6). We chose to evaluate 3 day eluates as burst release is a common phenomenon observed within the first 24–72 hr of polymer delivery, and to assess the short-term functionality of these fibers against HSV-2 infection. For an indication of long-term protection, we assessed the total ACV released into eluate after one month, and also between days 21–28 (during the 4th week of release) where typically little release is noted.

For all of these release time points, we showed that EFs maintain functional activity, making them potentially suitable for efficacious delivery regardless of administration time within a one month timeframe. Furthermore, the IC50s of these fibers were similar to free, transiently acting ACV confirming the bioactivity of our delivery vehicle after prolonged exposure to SVF. That is, EFs incubated in SVF for up to 28 days retained similar activity to free, freshly administered ACV. Together with loading and controlled release data, this suggests that these fibers have the potential to protect against HSV-2 infection for up to one month, with less frequent dosing than free ACV. Furthermore, by enabling prolonged release, we hypothesize that incorporated ACV will maintain activity more readily than free ACV over the course of one month *in vivo*. Last, we believe the dual-release capabilities at both early and sustained time points may impart versatility for administration options in our end application.

With these initial observations of EF antiviral efficacy *in vitro*, we hypothesized that the blank EFs alone (with no encapsulant) might serve as a protective barrier device, as EFs

have a similar porous morphology to mucus and exhibit low degradation after 28 days. Previous work has highlighted mucus as an innate protective mechanism to decrease virus transport and hence infection. With pore sizes larger than HSV (HSV ~170nm), cervicovaginal mucus (CVM) has been studied for its ability to hinder virus transport. In fact, CVM is believed to provide innate protection against infection primarily through mucoadhesive mucin interactions, by physically decreasing the flux of pathogens to the underlying epithelium [94–96]. Similarly, we suggest that polymeric EFs, with similar porous networks, may provide a first layer of physical protection to virus entry and inhibition. While we examined an ideal scenario of administering HSV-2 atop fibers suspended in a transwell membrane, we expect that fiber tortuosity and interaction with the fibers may contribute to this decrease in penetration we observe. Indeed, when the luminal surfaces of EFs were administered the highest concentration of virus used in plaque assays, and placed in physical contact with media and cells below, both PLGA and PLCL EFs served as barriers to infection over the course of 2–3 days (Figure 7). Correlating these results with pore size and calculated porosity, we observed that the average pore size is much larger than virus. However, each fiber is comprised of multiple layers of fibers, likely creating a tortuous network for virus transport. We believe, virus may be hindered between layers, perhaps similar to virus-mucosa studies, where virus inhibition is dependent on electrostatic and hydrophobic interactions, instead of pore size [95, 97]. Overall these results suggest that EFs might be designed for potential use as a physical barrier device at least pericoitally in addition to their ability to encapsulate and sustainably release antivirals. However to validate the exact mechanism of the virus and fiber interaction, future mechanistic studies should be conducted.

In addition to our data that support the sustained-delivery and high loading of ACV PLGA and PLCL EFs, it is important for microbicide delivery vehicles to demonstrate biocompatibility early in the early design and testing phases. Importantly here, high *in vitro* cell viability was demonstrated (Figure 8). We selected a dose of 1 mg/mL to be tested *in vitro*, as clinical studies have demonstrated *in vivo* administration of intravaginal rings or comparable delivery technologies spanning 1 to greater than 100 mg in the female reproductive tract (~2–3 mL volume) [45, 98–101]. While in a cell-based system, we felt that 1 mg/mL was a sufficiently high concentration to provide an indication of toxicity, future explant and *in vivo* studies will evaluate increased concentrations relevant to translation in each system.

In future work we plan to build upon this initial platform to advance this work against multiple STIs and in *in vivo* models. In particular, we are interested in formulating new polymeric blends to address and decrease burst release by tuning release properties. These could be in the form of either fibers comprised of a polymer blend, or composite scaffolds of mixed fiber types. Ideally, a composite or blended system that has both hydrophilic and hydrophobic properties would be desirable to tune release. In addition to formulation changes, we may also consider physical changes to our fiber morphology. For example, we could use a different electrospinning technique to create more of a core-shell structure, or a layering approach to minimize initial diffusion. For our delivery goals, however, it is desirable to have release spanning the period of initial insertion through one month, so some moderate level of burst release is desired. In addition to this work, it would be desirable to

conduct additional mechanical tests as they relate to fibers of varying porosity and thickness, to better understand how these properties may relate to both virus protection and user experience for translational applications.

5. Conclusions

To our knowledge, there are few delivery platforms currently available for long-term microbicide applications, and none-to-date that use EFs as a physicochemical barrier against HSV-2 infection. Here we synthesized, characterized, and tested various formulations of PLGA and PLCL EFs to demonstrate that these EFs have the potential to potently protect against HSV-2 infection *in vitro*. Our data support that PLGA and PLCL EFs exhibit sustained-delivery, high loading of ACV, and importantly, strong *in vitro* cell viability. Furthermore, all fiber eluates achieved comparable bioactivity to free ACV demonstrating the ability of PLGA and PLCL EFs to: safely encapsulate ACV, maintain bioactivity in SVF for up to 28 days, and provide corresponding short- and long-term protection against HSV-2 infection *in vitro*. Based on these results, combined with their potent *in vitro* efficacy at different durations of EF release, we expect either PLGA or PLCL EFs may be utilized to combat HSV-2 infection, while having broader potential against a diversity of infections.

Supplementary Material

Refer to Web version on PubMed Central for supplementary material.

Acknowledgments

We are greatly appreciative to our fellow University of Louisville colleagues for the use of their equipment. We thank Dr. Stuart Williams III for generously allowing us to use his electrospinning apparatus; Dr. Martin O'Toole for use of his ZetaPALS for conductivity measurements; Dr. Thomas Berfield for use of his tensile testing machine, and Dr. Eric Berson for the use of his rheometer.

References

1. Looker KJ, Garnett GP, Schmid GP. An estimate of the global prevalence and incidence of herpes simplex virus type 2 infection. Bull World Health Organ. 2008; 86(10):805–12. [PubMed: 18949218]
2. Xu F, Schillinger JA, Sternberg MR, Johnson RE, Lee FK, Nahmias AJ, et al. Seroprevalence and coinfection with herpes simplex virus type 1 and type 2 in the United States, 1988–1994. The Journal of infectious diseases. 2002; 185(8):1019–24. [PubMed: 11930310]
3. Ndesendo VM, Pillay V, Choonara YE, Buchmann E, Bayever DN, Meyer LC. A review of current intravaginal drug delivery approaches employed for the prophylaxis of HIV/AIDS and prevention of sexually transmitted infections. AAPS PharmSciTech. 2008; 9(2):505–20. [PubMed: 18431651]
4. Koelle DM, Corey L. Herpes simplex: insights on pathogenesis and possible vaccines. Annual review of medicine. 2008; 59:381–95.
5. Rohan LC, Sassi AB. Vaginal drug delivery systems for HIV prevention. Aaps J. 2009; 11(1):78–87. [PubMed: 19194802]
6. Looker KJ, Magaret AS, Turner KM, Vickerman P, Gottlieb SL, Newman LM. Global estimates of prevalent and incident herpes simplex virus type 2 infections in 2012. PloS one. 2015; 10(1):e114989.doi: 10.1371/journal.pone.0114989 [PubMed: 25608026]
7. Corey L, Wald A, Celum CL, Quinn TC. The effects of herpes simplex virus-2 on HIV-1 acquisition and transmission: a review of two overlapping epidemics. Journal of acquired immune deficiency syndromes. 2004; 35(5):435–45. [PubMed: 15021308]

8. Dasgupta G, Chentoufi AA, Nesburn AB, Wechsler SL, BenMohamed L. New concepts in herpes simplex virus vaccine development: notes from the battlefield. Expert Rev Vaccines. 2009; 8(8): 1023–35. [PubMed: 19627185]
9. Serwadda D, Gray RH, Sewankambo NK, Wabwire-Mangen F, Chen MZ, Quinn TC, et al. Human immunodeficiency virus acquisition associated with genital ulcer disease and herpes simplex virus type 2 infection: a nested case-control study in Rakai, Uganda. The Journal of infectious diseases. 2003; 188(10):1492–7. [PubMed: 14624374]
10. Sobngwi-Tambekou J, Taljaard D, Lissouba P, Zarca K, Puren A, Lagarde E, et al. Effect of HSV-2 serostatus on acquisition of HIV by young men: results of a longitudinal study in Orange Farm, South Africa. The Journal of infectious diseases. 2009; 199(7):958–64. [PubMed: 19220143]
11. Tobian AA, Quinn TC. Herpes simplex virus type 2 and syphilis infections with HIV: an evolving synergy in transmission and prevention. Curr Opin HIV AIDS. 2009; 4(4):294–9. [PubMed: 19532067]
12. Wald A, Link K. Risk of human immunodeficiency virus infection in herpes simplex virus type 2-seropositive persons: a meta-analysis. The Journal of infectious diseases. 2002; 185(1):45–52. [PubMed: 11756980]
13. Berer M. Dual protection: more needed than practised or understood. Reprod Health Matters. 2006; 14(28):162–70. Epub 2006/11/15. DOI: 10.1016/S0968-8080(06)28262-4 [PubMed: 17101435]
14. Brady M. Preventing sexually transmitted infections and unintended pregnancy, and safeguarding fertility: triple protection needs of young women. Reprod Health Matters. 2003; 11(22):134–41. Epub 2004/01/08. [PubMed: 14708404]
15. Bull SS, Shlay JC. Promoting “dual protection” from pregnancy and sexually transmitted disease: a social ecological approach. Health Promot Pract. 2005; 6(1):72–80. Epub 2004/12/03. DOI: 10.1177/1524839903259308 [PubMed: 15574531]
16. Cates W Jr, Steiner MJ. Dual protection against unintended pregnancy and sexually transmitted infections: what is the best contraceptive approach? Sexually transmitted diseases. 2002; 29(3): 168–74. Epub 2002/03/05. [PubMed: 11875378]
17. Chandran P, Kabir SN. Dual action microbicides: reappraisal of their roles in contraceptive research. Reprod Biomed Online. 2010; 20(1):103–13. Epub 2010/02/18. DOI: 10.1016/j.rbmo.2009.10.018 [PubMed: 20158995]
18. Karim QA, Karim SSA, Frohlich JA, Grobler AC, Baxter C, Mansoor LE, et al. Effectiveness and Safety of Tenofovir Gel, an Antiretroviral Microbicide, for the Prevention of HIV Infection in Women. Science. 2010; 329(5996):1168–74. DOI: 10.1126/science.1193748 [PubMed: 20643915]
19. CONRAD. CONRAD: Clinical Trials. Antiretrovirals as Microbides: Tenofovir (TFV). http://www.conrad.org/microbicides-trials.html2014. Available from: http://www.conrad.org/microbicides-trials.html
20. IPM. International Partnership for Microbicides Webpage. http://www.ipmglobal.org/2014. Available from: http://www.ipmglobal.org/
21. MTN. MTN statement on decision to discontinue use of oral tenofovir tablets in VOICE, a major HIV prevention study in women. 2011
22. Dapivirine vaginal ring helped protect women against HIV in ASPIRE Phase III trial [Internet]. Feb 22.2016 2016 http://www.mtnstopshiv.org/node/7229. Available from: http://www.mtnstopshiv.org/node/7229.
23. Network MT. MTN: Microbicide Trials Network - Studies. http://www.mtnstopshiv.org/studies2014. Available from: http://www.mtnstopshiv.org/studies
24. Abdool Karim Q, Abdool Karim SS, Frohlich JA, Grobler AC, Baxter C, Mansoor LE, et al. Effectiveness and safety of tenofovir gel, an antiretroviral microbicide, for the prevention of HIV infection in women. Science. 2010; 329(5996):1168–74. [PubMed: 20643915]
25. Gengiah TN, Abdool Karim Q. Implementing microbicides in low-income countries. Best practice & research Clinical obstetrics & gynaecology. 2012; 26(4):495–501. Epub 2012/04/14. DOI: 10.1016/j.bpobgyn.2012.02.004 [PubMed: 22498040]
26. Gengiah TN, Baxter C, Mansoor LE, Kharsany AB, Abdool Karim SS. A drug evaluation of 1% tenofovir gel and tenofovir disoproxil fumarate tablets for the prevention of HIV infection. Expert

Opin Investig Drugs. 2012; 21(5):695–715. Epub 2012/03/08. DOI: 10.1517/13543784.2012.667072

27. Malcolm RK, Edwards KL, Kiser P, Romano J, Smith TJ. Advances in microbicide vaginal rings. Antiviral research. 2010; 88(Suppl 1):S30–9. Epub 2010/12/09. DOI: 10.1016/j.antiviral.2010.09.003 [PubMed: 21109066]
28. Montgomery ET, van der Straten A, Cheng H, Wegner L, Masenga G, von Mollendorf C, et al. Vaginal ring adherence in sub-Saharan Africa: expulsion, removal, and perfect use. AIDS and behavior. 2012; 16(7):1787–98. DOI: 10.1007/s10461-012-0248-4 [PubMed: 22790902]
29. Population Council. Microbicides and Multipurpose Prevention Technologies. http://www.popcouncil.org/research2014. Available from: http://www.popcouncil.org/research
30. IMPT for Reproductive Health. MPT Product Development Database. 2014. http://mpts101.org/mpt-database/product-page/35-candidate-single-indication-agents-for-mpts/anti-hiv-topical-rings/87-maraviroc-international-partnership-for-microbicides-ipm-usaid-niaid-daids-vaginal-ring-ivr-hivAvailable from: http://mpts101.org/mpt-database/product-page/35-candidate-single-indication-agents-for-mpts/anti-hiv-topical-rings/87-maraviroc-international-partnership-for-microbicides-ipm-usaid-niaid-daids-vaginal-ring-ivr-hiv
31. AIDS Info. Clinical Trial Search Results. http://aidsinfo.nih.gov/clinical-trials/search/q/1/category/59/prevention-research/63/microbicides2014. Available from: http://aidsinfo.nih.gov/clinical-trials/search/q/1/category/59/prevention-research/63/microbicides
32. AVAC. AVAC: Trial Summary Table. http://www.avac.org/trial-summary-table/microbicides2014. Available from: http://www.avac.org/trial-summary-table/microbicides
33. ClinicalTrials.gov. ClinicalTrials.gov: Safety and Acceptability Study of Oral Emtricitabine/Tenofovir Disoproxil Fumarate Tablet and Rectally-Applied Tenofovir Reduced-Glycerin 1% Gel. http://clinicaltrials.gov/show/NCT016872182014. Available from: http://clinicaltrials.gov/show/NCT01687218
34. MTN statement on decision to discontinue tenofovir gel in VOICE, a major HIV prevention study in women. [Internet]. Nov.2011 2011 http://www.mtnstopshiv.org/node/3909. posting date.
35. Steinbach JM. Protein and oligonucleotide delivery systems for vaginal microbicides against viral STIs. Cellular and molecular life sciences : CMLS. 2015; 72(3):469–503. DOI: 10.1007/s00018-014-1756-3 [PubMed: 25323132]
36. Schwartz JL, Mauck C, Lai JJ, Creinin MD, Brache V, Ballagh SA, et al. Fourteen-day safety and acceptability study of 6% cellulose sulfate gel: a randomized double-blind Phase I safety study. Contraception. 2006; 74(2):133–40. DOI: 10.1016/j.contraception.2006.02.008 [PubMed: 16860051]
37. Schwartz JL, Ballagh SA, Kwok C, Mauck CK, Weiner DH, Rencher WF, et al. Fourteen-day safety and acceptability study of the universal placebo gel. Contraception. 2007; 75(2):136–41. DOI: 10.1016/j.contraception.2006.09.003 [PubMed: 17241844]
38. Coetzee N, Blanchard K, Ellertson C, Hoosen AA, Friedland B. Acceptability and feasibility of Micralax applicators and of methyl cellulose gel placebo for large-scale clinical trials of vaginal microbicides. Aids. 2001; 15(14):1837–42. [PubMed: 11579246]
39. Bentley ME, Fullem AM, Tolley EE, Kelly CW, Jogelkar N, Srirak N, et al. Acceptability of a microbicide among women and their partners in a 4-country phase I trial. American journal of public health. 2004; 94(7):1159–64. [PubMed: 15226137]
40. Gross M, Celum CL, Tabet SR, Kelly CW, Coletti AS, Chesney MA. Acceptability of a bioadhesive nonoxynol-9 gel delivered by an applicator as a rectal microbicide. Sexually transmitted diseases. 1999; 26(10):572–8. [PubMed: 10560721]
41. Holt BY, Morwitz VG, Ngo L, Harrison PF, Whaley KJ, Pettifor A, et al. Microbicide preference among young women in California. Journal of women's health. 2006; 15(3):281–94. DOI: 10.1089/jwh.2006.15.281
42. Malonza IM, Mirembe F, Nakabiito C, Odusoga LO, Osinupebi OA, Hazari K, et al. Expanded Phase I safety and acceptability study of 6% cellulose sulfate vaginal gel. Aids. 2005; 19(18):2157–63. [PubMed: 16284466]

43. Buckheit RW Jr, Watson KM, Morrow KM, Ham AS. Development of topical microbicides to prevent the sexual transmission of HIV. Antiviral research. 2010; 85(1):142–58. DOI: 10.1016/j.antiviral.2009.10.013 [PubMed: 19874851]
44. Malcolm RK, Fetherston SM, McCoy CF, Boyd P, Major I. Vaginal rings for delivery of HIV microbicides. Int J Womens Health. 2012; 4:595–605. Epub 2012/12/04. DOI: 10.2147/IJWH.S36282 [PubMed: 23204872]
45. Smith JM, Rastogi R, Teller RS, Srinivasan P, Mesquita PM, Nagaraja U, et al. Intravaginal ring eluting tenofovir disoproxil fumarate completely protects macaques from multiple vaginal simian-HIV challenges. Proceedings of the National Academy of Sciences of the United States of America. 2013; 110(40):16145–50. DOI: 10.1073/pnas.1311355110 [PubMed: 24043812]
46. Mesquita PM, Srinivasan P, Johnson TJ, Rastogi R, Evans-Strickfaden T, Kay MS, et al. Novel preclinical models of topical PrEP pharmacodynamics provide rationale for combination of drugs with complementary properties. Retrovirology. 2013; 10:113.doi: 10.1186/1742-4690-10-113 [PubMed: 24156604]
47. Friend DR. Drug delivery in multiple indication (multipurpose) prevention technologies: systems to prevent HIV-1 transmission and unintended pregnancies or HSV-2 transmission. Expert opinion on drug delivery. 2012; 9(4):417–27. Epub 2012/03/06. DOI: 10.1517/17425247.2012.668183 [PubMed: 22385316]
48. Mesquita PM, Rastogi R, Segarra TJ, Teller RS, Torres NM, Huber AM, et al. Intravaginal ring delivery of tenofovir disoproxil fumarate for prevention of HIV and herpes simplex virus infection. The Journal of antimicrobial chemotherapy. 2012; 67(7):1730–8. DOI: 10.1093/jac/dks097 [PubMed: 22467632]
49. Asvadi NH, Dang NT, Davis-Poynter N, Coombes AG. Evaluation of microporous polycaprolactone matrices for controlled delivery of antiviral microbicides to the female genital tract. Journal of materials science Materials in medicine. 2013; 24(12):2719–27. DOI: 10.1007/s10856-013-5010-6 [PubMed: 23892484]
50. Huang C, Soenen SJ, van Gulck E, Vanham G, Rejman J, Van Calenbergh S, et al. Electrospun cellulose acetate phthalate fibers for semen induced anti-HIV vaginal drug delivery. Biomaterials. 2012; 33(3):962–9. DOI: 10.1016/j.biomaterials.2011.10.004 [PubMed: 22018388]
51. Krogstad EA, Woodrow KA. Manufacturing scale-up of electrospun poly(vinyl alcohol) fibers containing tenofovir for vaginal drug delivery. International journal of pharmaceutics. 2014; 475(1–2):282–91. DOI: 10.1016/j.ijpharm.2014.08.039 [PubMed: 25169075]
52. Blakney AK, Ball C, Krogstad EA, Woodrow KA. Electrospun fibers for vaginal anti-HIV drug delivery. Antiviral research. 2013; 100(Suppl):S9–16. DOI: 10.1016/j.antiviral.2013.09.022 [PubMed: 24188701]
53. Ball C, Krogstad E, Chaowanachan T, Woodrow KA. Drug-eluting fibers for HIV-1 inhibition and contraception. PloS one. 2012; 7(11):e49792.doi: 10.1371/journal.pone.0049792 [PubMed: 23209601]
54. Huang C, Soenen SJ, van Gulck E, Rejman J, Vanham G, Lucas B, et al. Electrospun polystyrene fibers for HIV entrapment. Polymers Advanced Technologies. 2014; 25(8):827–34.
55. Ball C, Woodrow KA. Electrospun solid dispersions of Maraviroc for rapid intravaginal preexposure prophylaxis of HIV. Antimicrobial agents and chemotherapy. 2014; 58(8):4855–65. DOI: 10.1128/AAC.02564-14 [PubMed: 24913168]
56. Blakney AK, Krogstad EA, Jiang YH, Woodrow KA. Delivery of multipurpose prevention drug combinations from electrospun nanofibers using composite microarchitectures. International journal of nanomedicine. 2014; 9:2967–78. DOI: 10.2147/IJN.S61664 [PubMed: 24971008]
57. Liang D, Hsiao BS, Chu B. Functional electrospun nanofibrous scaffolds for biomedical applications. Advanced drug delivery reviews. 2007; 59(14):1392–412. DOI: 10.1016/j.addr.2007.04.021 [PubMed: 17884240]
58. Chou SF, Carson D, Woodrow KA. Current strategies for sustaining drug release from electrospun nanofibers. Journal of controlled release : official journal of the Controlled Release Society. 2015; 220(Pt B):584–91. DOI: 10.1016/j.jconrel.2015.09.008 [PubMed: 26363300]

59. Zamani M, Prabhakaran MP, Ramakrishna S. Advances in drug delivery via electrospun and electrosprayed nanomaterials. International journal of nanomedicine. 2013; 8:2997–3017. DOI: 10.2147/IJN.S43575 [PubMed: 23976851]
60. Ball C, Chou SF, Jiang Y, Woodrow KA. Coaxially electrospun fiber-based microbicides facilitate broadly tunable release of maraviroc. Materials science & engineering C, Materials for biological applications. 2016; 63:117–24. DOI: 10.1016/j.msec.2016.02.018 [PubMed: 27040202]
61. Carson D, Jiang Y, Woodrow KA. Tunable Release of Multiclass Anti-HIV Drugs that are Water-Soluble and Loaded at High Drug Content in Polyester Blended Electrospun Fibers. Pharmaceutical research. 2016; 33(1):125–36. DOI: 10.1007/s11095-015-1769-0 [PubMed: 26286184]
62. Grooms TN, Vuong HR, Tyo KM, Malik DA, Sims LB, Whittington CP, et al. Griffithsin-Modified Electrospun Fibers as a Delivery Scaffold to Prevent HIV Infection. Antimicrobial agents and chemotherapy. 2016; doi: 10.1128/AAC.00956-16
63. Steinbach JM, Weller CE, Booth CJ, Saltzman WM. Polymer nanoparticles encapsulating siRNA for treatment of HSV-2 genital infection. Journal of controlled release : official journal of the Controlled Release Society. 2012; 162(1):102–10. Epub 2012/06/19. DOI: 10.1016/j.jconrel.2012.06.008 [PubMed: 22705461]
64. Ping L, Bin D. Applications of Electrospun Fibers. Recent Patents on Nanotechnology. 2008; 2(3)
65. Abedalwafa M, Wang FJ, Wang L, Li CJ. Biodegradable Poly-Epsilon-Caprolactone (Pcl) for Tissue Engineering Applications: A Review. Rev Adv Mater Sci. 2013; 34(2):123–40.
66. Sabir MI, Xu XX, Li L. A review on biodegradable polymeric materials for bone tissue engineering applications. J Mater Sci. 2009; 44(21):5713–24. DOI: 10.1007/s10853-009-3770-7
67. Gentile P, Chiono V, Carmagnola I, Hatton PV. An overview of poly(lactic-co-glycolic) acid (PLGA)-based biomaterials for bone tissue engineering. International journal of molecular sciences. 2014; 15(3):3640–59. DOI: 10.3390/ijms15033640 [PubMed: 24590126]
68. Makadia HK, Siegel SJ. Poly Lactic-co-Glycolic Acid (PLGA) as Biodegradable Controlled Drug Delivery Carrier. Polymers. 2011; 3(3):1377–97. DOI: 10.3390/polym3031377 [PubMed: 22577513]
69. Singh O, Garg T, Rath G, Goyal AK. Microbicides for the Treatment of Sexually Transmitted HIV Infections. Journal of Pharmaceutics. 2014; 2014(352425)
70. Gao P, Nie X, Zou M, Shi Y, Cheng G. Recent advances in materials for extended-release antibiotic delivery system. The Journal of antibiotics. 2011; 64(9):625–34. DOI: 10.1038/ja.2011.58 [PubMed: 21811264]
71. Sartoneva R, Haaparanta AM, Lahdes-Vasama T, Mannerstrom B, Kellomaki M, Salomaki M, et al. Characterizing and optimizing poly-L-lactide-co-epsilon-caprolactone membranes for urothelial tissue engineering. J R Soc Interface. 2012; 9(77):3444–54. DOI: 10.1098/rsif.2012.0458 [PubMed: 22896571]
72. Jeong SI, Kim BS, Lee YM, Ihn KJ, Kim SH, Kim YH. Morphology of elastic poly(L-lactide-co-epsilon-caprolactone) copolymers and in vitro and in vivo degradation behavior of their scaffolds. Biomacromolecules. 2004; 5(4):1303–9. DOI: 10.1021/bm049921i [PubMed: 15244444]
73. Owen DH, Katz DF. A vaginal fluid simulant. Contraception. 1999; 59(2):91–5. [PubMed: 10361623]
74. Dierickx W. Opening size determination of technical textiles used in agricultural applications. Geotext Geomembranes. 1999; 17(4):231–45.
75. Gu XH, Song X, Shao CH, Zeng P, Lu XK, Shen XY, et al. Electrospinning of poly(butylene-carbonate):Effect of Solvents on the Properties of the Nanofibers Film. Int J Electrochem Sci. 2014; 9:8045–56.
76. Skotheim, TA., Reynolds, J., editors. Conjugated Polymers, Processing and Applications. CRC Press; 2007. Handbook of Conducting Polymers Third Edition.
77. SmartMeasurement(™). SmartMeasurement Calculators and Utilities - Conductivity. http://www.smartmeasurement.com/calculators-utilities/conductivity2016. Available from: http://www.smartmeasurement.com/calculators-utilities/conductivity

78. Taminco. Dimethylformamide Technical Data Sheet. http://colonialchemicals.com/uploads/Products/DMF/DMF_Tech.pdf2005. Available from: http://colonialchemicals.com/uploads/Products/DMF/DMF_Tech.pdf

79. Azimi B, Nourpanah P, Rabiee M, Arbab S. Poly (lactide -co- glycolide) Fiber: An Overview. Journal of Engineered Fibers and Fabrics. 2014; 9(1):47–66.

80. Pillay V, Dott C, Choonara YE, Tyagi C, Tomar L, Kumar P, et al. A Review of the Effect of Processing Variables on the Fabrication of Electrospun Nanofibers for Drug Delivery Applications. J Nanomater. 2013; Artn 789289. doi: 10.1155/2013/789289

81. Jarusuwannapoom T, Hongroijanawiwat W, Jitjaicham S, Wannatong L, Nithitanakul M, Pattamaprom C, et al. Effect of solvents on electro-spinnability of polystyrene solutions and morphological appearance of resulting electrospun polystyrene fibers. Eur Polym J. 2005; 41(3): 409–21. DOI: 10.1016/j.eurpolymj.2004.10.010

82. Qian YF, Su Y, Li XQ, Wang HS, He CL. Electrospinning of Polymethyl Methacrylate Nanofibres in Different Solvents. Iran Polym J. 2010; 19(2):123–9.

83. Mo XM, Xu CY, Kotaki M, Ramakrishna S. Electrospun P(LLA-CL) nanofiber: a biomimetic extracellular matrix for smooth muscle cell and endothelial cell proliferation. Biomaterials. 2004; 25(10):1883–90. [PubMed: 14738852]

84. Gu XH, Song X, Shao CH, Zeng P, Lu XK, Shen XY, et al. Electrospinning of poly(butylene-carbonate): Effect of Solvents on the Properties of the Nanofibers Film. Int J Electrochem Sc. 2014; 9(12):8045–56.

85. Dalton, LR. Dalton Research Group Website: Dielectric Chart. http://depts.washington.edu/eooptic/linkfiles/dielectric_chart%5B1%5D.pdf2016. Available from: http://depts.washington.edu/eooptic/linkfiles/dielectric_chart%5B1%5D.pdf

86. Leonard, M. MJLPHD: Solvent of the Week. http://www.mjlphd.net/solvent-of-the-week.html2016. Available from: http://www.mjlphd.net/solvent-of-the-week.html

87. Haider A, Haider S, Kang I. A comprehensive review summarizing the effect of electrospinning parameters and potential applications of nanofibers in biomedical and biotechnology. Arabian Journal of Chemistry. 2015 in press.

88. Hartman O, Zhang C, Adams EL, Farach-Carson MC, Petrelli NJ, Chase BD, et al. Biofunctionalization of electrospun PCL-based scaffolds with perlecan domain IV peptide to create a 3-D pharmacokinetic cancer model. Biomaterials. 2010; 31(21):5700–18. DOI: 10.1016/j.biomaterials.2010.03.017 [PubMed: 20417554]

89. Reddy SMM, Shanmugam G, Mandal AB. 1,1,1,3,3,3-Hexafluoro-2-propanol and 2,2,2-trifluoroethanol solvents induce self-assembly with different surface morphology in an aromatic dipeptide. Org Biomol Chem. 2014; 12(32):6181–9. DOI: 10.1039/c4ob00821a [PubMed: 24999600]

90. Ajalloueian F, Tavanai H, Hilborn J, Donzel-Gargand O, Leifer K, Wickham A, et al. Emulsion Electrospinning as an Approach to Fabricate PLGA/Chitosan Nanofibers for Biomedical Applications. Biomed Res Int. 2014; Artn 475280. doi: 10.1155/2014/475280

91. Liao YL, Zhang LF, Gao Y, Zhu ZT, Fong H. Preparation, characterization, and encapsulation/release studies of a composite nanofiber mat electrospun from an emulsion containing poly(lactic-co-glycolic acid). Polymer. 2008; 49(24):5294–9. DOI: 10.1016/j.polymer.2008.09.045 [PubMed: 19907634]

92. Chew SY, Hufnagel TC, Lim CT, Leong KW. Mechanical properties of single electrospun drug-encapsulated nanofibres. Nanotechnology. 2006; 17(15):3880–91. DOI: 10.1088/0957-4484/17/15/045 [PubMed: 19079553]

93. Jia X, Zhao C, Li P, Zhang H, Huang Y, Li H, et al. Sustained release of VEGF by coaxial electrospun dextran/PLGA fibrous membranes in vascular tissue engineering. J Biomater Sci Polym Ed. 2011; 22(13):1811–27. DOI: 10.1163/092050610X528534 [PubMed: 20961491]

94. Lai SK, Wang YY, Hanes J. Mucus-penetrating nanoparticles for drug and gene delivery to mucosal tissues. Advanced drug delivery reviews. 2009; 61(2):158–71. Epub 2009/01/10. DOI: 10.1016/j.addr.2008.11.002 [PubMed: 19133304]

95. Lai SK, Wang YY, Hida K, Cone R, Hanes J. Nanoparticles reveal that human cervicovaginal mucus is riddled with pores larger than viruses. Proceedings of the National Academy of Sciences

of the United States of America. 2010; 107(2):598–603. Epub 2009/12/19. DOI: 10.1073/pnas.0911748107 [PubMed: 20018745]

96. Lai SK, Wang YY, Wirtz D, Hanes J. Micro- and macrorheology of mucus. Advanced drug delivery reviews. 2009; 61(2):86–100. Epub 2009/01/27. DOI: 10.1016/j.addr.2008.09.012 [PubMed: 19166889]
97. Lai SK, O'Hanlon DE, Harrold S, Man ST, Wang YY, Cone R, et al. Rapid transport of large polymeric nanoparticles in fresh undiluted human mucus. Proceedings of the National Academy of Sciences of the United States of America. 2007; 104(5):1482–7. DOI: 10.1073/pnas.0608611104 [PubMed: 17244708]
98. Johnson TJ, Srinivasan P, Albright TH, Watson-Buckheit K, Rabe L, Martin A, et al. Safe and sustained vaginal delivery of pyrimidinedione HIV-1 inhibitors from polyurethane intravaginal rings. Antimicrobial agents and chemotherapy. 2012; 56(3):1291–9. DOI: 10.1128/AAC.05721-11 [PubMed: 22155820]
99. Moss JA, Malone AM, Smith TJ, Butkyavichene I, Cortez C, Gilman J, et al. Safety and pharmacokinetics of intravaginal rings delivering tenofovir in pig-tailed macaques. Antimicrobial agents and chemotherapy. 2012; 56(11):5952–60. DOI: 10.1128/AAC.01198-12 [PubMed: 22964245]
100. Moss JA, Malone AM, Smith TJ, Kennedy S, Kopin E, Nguyen C, et al. Simultaneous delivery of tenofovir and acyclovir via an intravaginal ring. Antimicrobial agents and chemotherapy. 2012; 56(2):875–82. Epub 2011/11/30. DOI: 10.1128/AAC.05662-11 [PubMed: 22123689]
101. MTN. Microbicide Trials Network Studies. http://www.mtnstopshiv.org/studies [cited 2016]. Available from: http://www.mtnstopshiv.org/studies

Highlights

- PLGA and PLCL EFs exhibit sustained-delivery of ACV through one month.
- EFs exhibit high ACV encapsulation efficiency and *in vitro* biocompatibility.
- EFs serve as both physical and chemical barriers to HSV-2 infection.
- Potent *in vitro* efficacy is provided against HSV-2 infection for all formulations.
- HSV-2 protection is independent of administration times within one month.

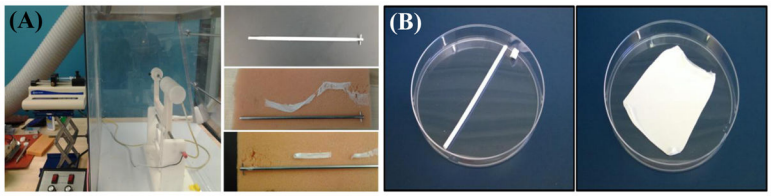

Figure 1.

(A) Schematic of the electrospinning apparatus and 4 mm mandrel. Various fiber sheets resulted from different solvents used during electrospinning, demonstrating no adhesion or adhesion to the mandrel. (B) Macroscale images of fiber sheets resulting from a 4 mm and 26 mm cylindrical mandrel, respectively.

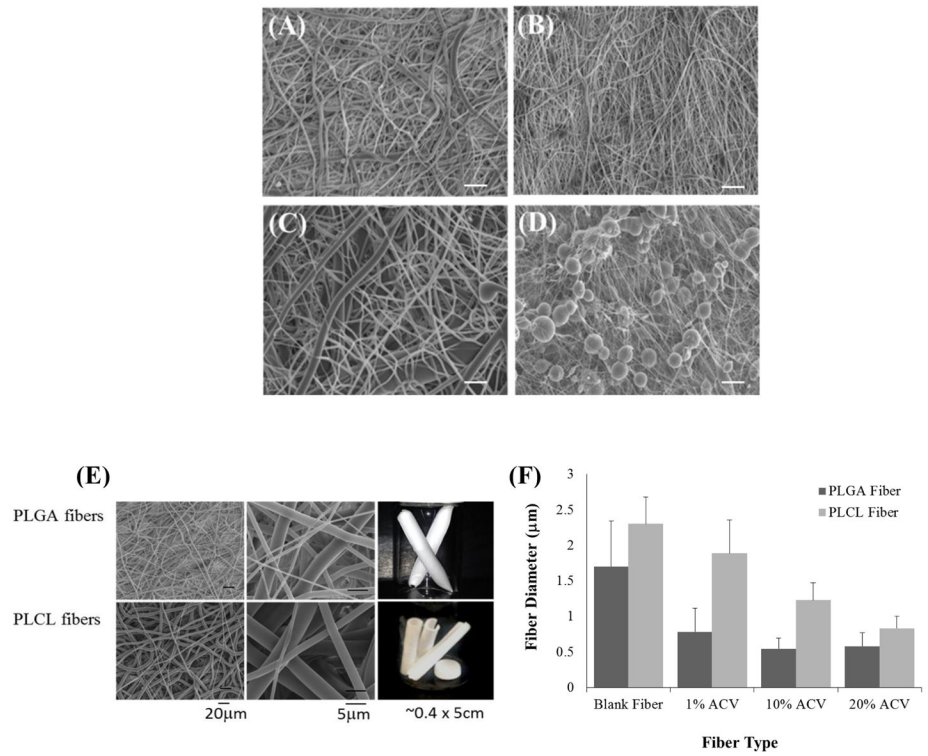

Figure 2.

SEM images of PLGA-only EFs formed with 4 different solvents: (A) HFIP, (B) 3:1 CF:DMF, (C) 9:1 CF:DMF, and (D) TFE. Scale bar = 20 μm. (E) SEM images and macroscale pictures comparing PLGA and PLCL EFs made with HFIP. Left column shows fiber microstructure, middle column shows higher magnification of the microstructure, and right column show the macroscale pictures of EFs. (F) The fiber diameters of HFIP PLGA and PLCL fibers, with and without different amounts of ACV added, were quantified with ImageJ.

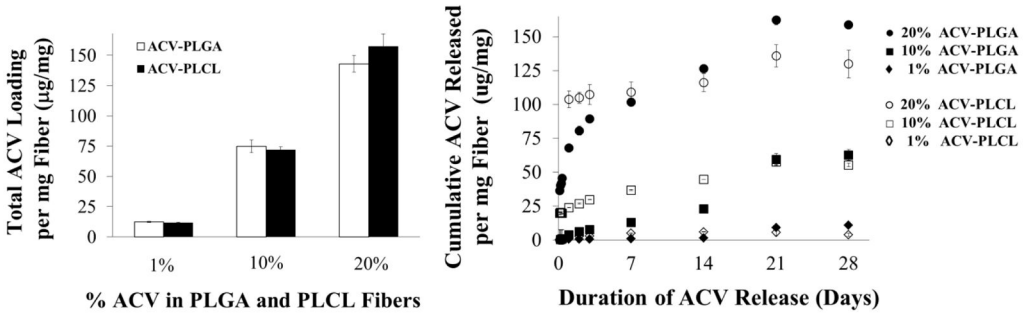

Figure 3.

(A) Fiber Loading: Mass of ACV incorporated within PLGA or PLCL EFs for 1, 10, and 20% loading. (B) Cumulative release of ACV from the 1, 10, and 20% ACV PLGA and PLCL EFs over 28 days. Cumulative release shown as µg of ACV released per mg of PLGA or PLCL fiber.

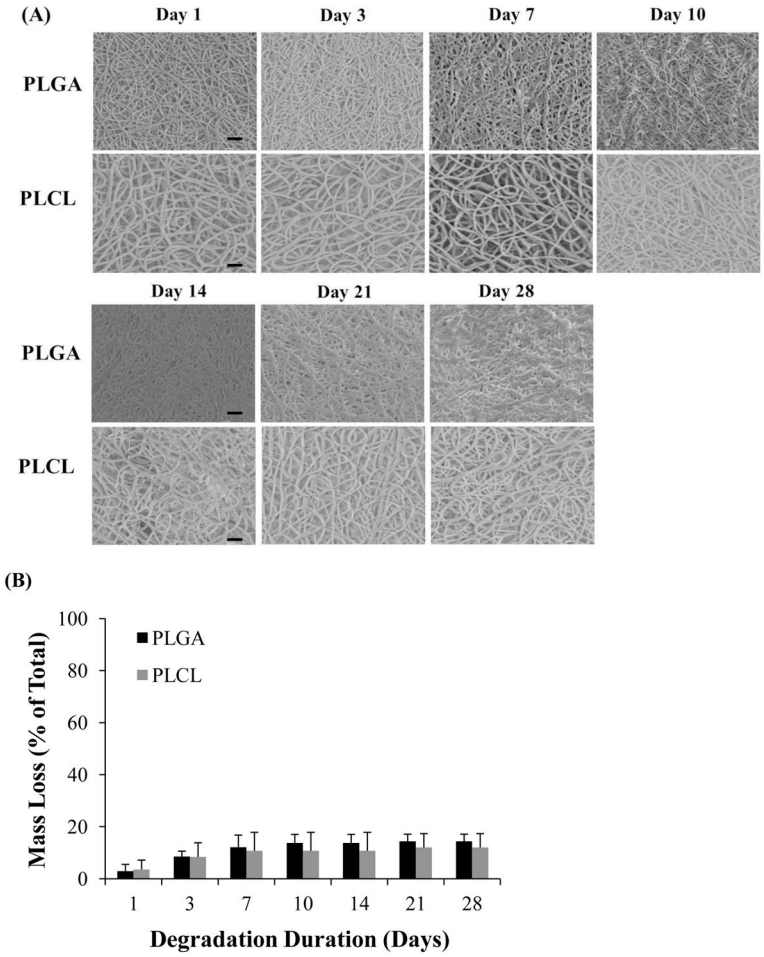

Figure 4.

(A) SEM microstructural degradation images of PLGA and PLCL EFs after 0, 3, 7, 10, 14, 21, and 28 days in SVF. Scale bar = 20 μm. (B) The corresponding percent mass loss relative to starting mass, resulting from 28 day degradation study. Only 12 to 14 % mass loss is observed after one month.

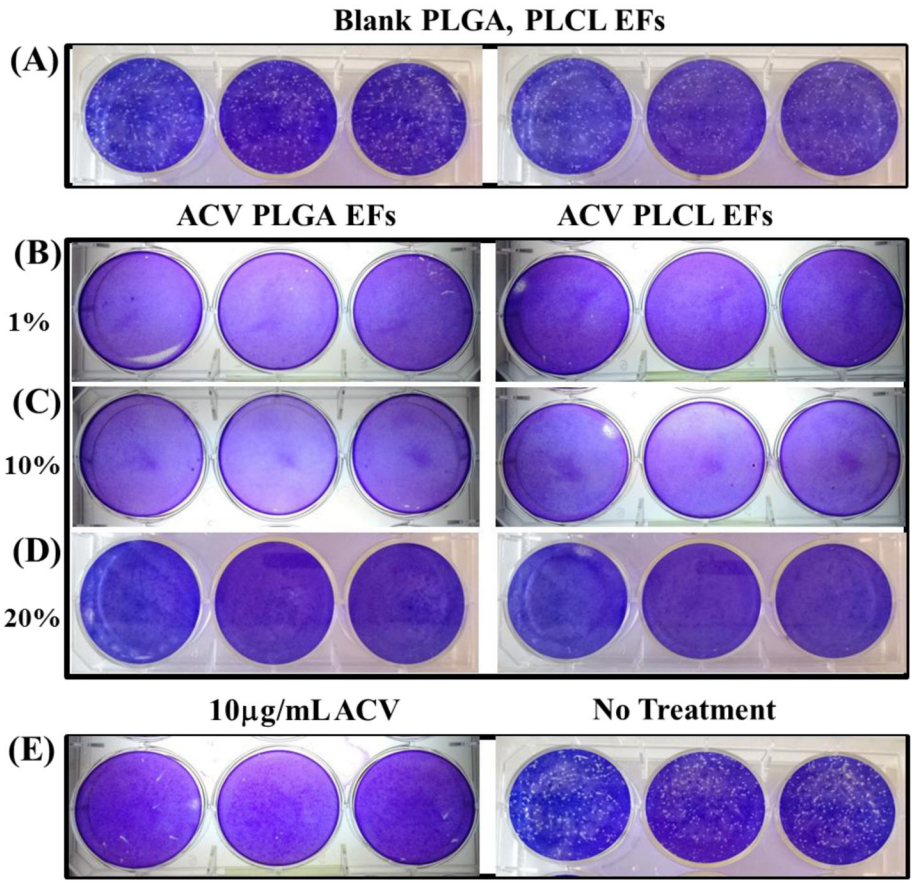

Figure 5.

Plaque assays show *in vitro* efficacy against HSV-2 infection after administration of PLGA and PLCL 1, 10, and 20% ACV EF eluates after 24 hour release from 1 mg/mL samples. Administration of: (A) blank PLGA and PLCL EFs (without ACV) results in greater than 260 plaques; (B–D) PLGA and PLCL EFs with increasing concentrations of ACV (1, 10, and 20% PLGA and PLCL ACV EFs) exhibit no plaque formation; and (E) controls of 10 μg/mL ACV (left) and no treatment (right) show negligible and greater than 260 plaques, respectively.

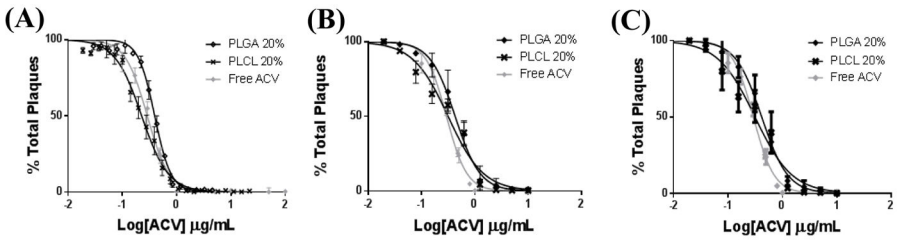

Figure 6.

Plaque assay HSV-2 inhibition curves resulting from administration of 20% ACV PLGA and PLCL fiber (10 mg/10 mL) eluates after: (A) 3 day, (B) 28 day, and (C) 21–28 day exposure to SVF, relative to free ACV.

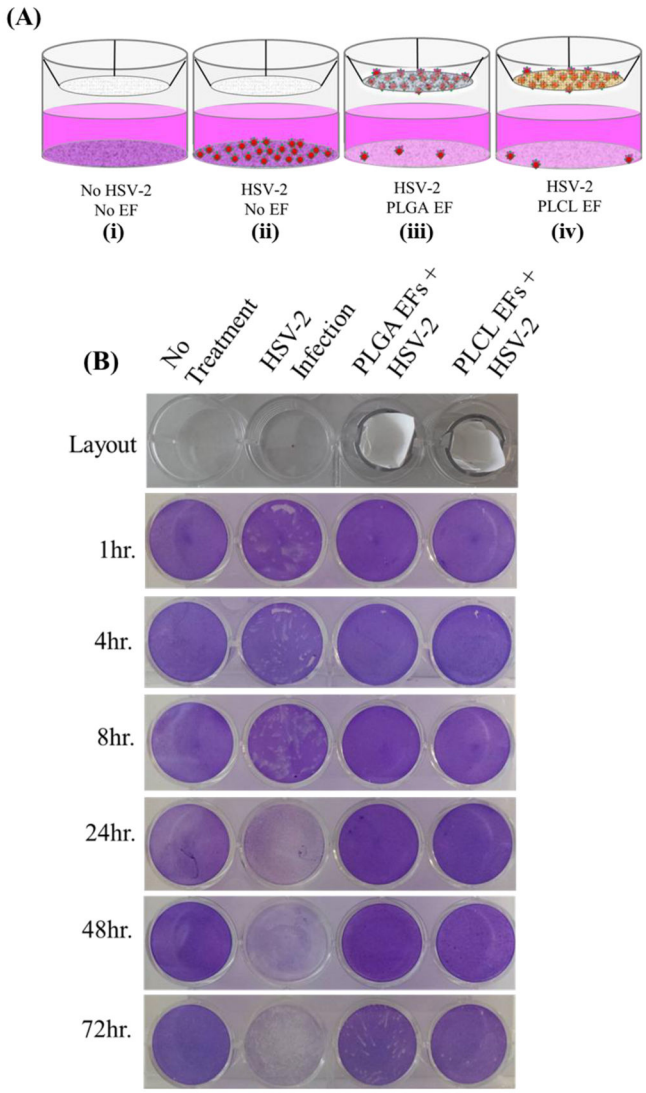

Figure 7.

(A) Schematic of HSV-2 penetration assay: (i) untreated, uninfected cells, (ii) untreated, HSV-2 infected cells, (iii) PLGA blank fiber-treated, HSV-2 infected cells, and (iv) PLCL blank fiber-treated cells, HSV-infected cells. (B) Plaque assay results from 0–72 hr incubation of virus, fiber, and cells.

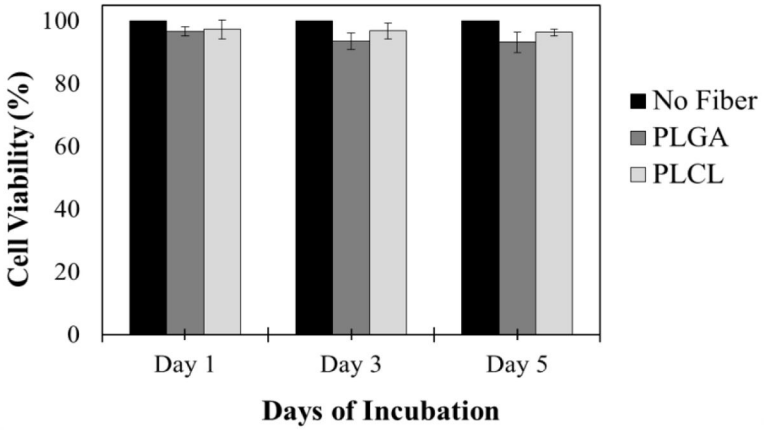

Figure 8.

HeLa cell viability after PLGA or PLCL fiber administration for 1, 3, and 5 days. PLGA and PLCL fibers are non-toxic at 1 mg/mL after these durations. Minimum viability after 5 days exposure is 93%.

Table 1

Quantification of average plaque number from Figure 5 plaque assay.

Sample	Average Plaque Number	Sample	Average Plaque Number
Bare PLGA	269 ± 6	**Bare PLCL**	261 ± 7
1% ACV PLGA	0	**1% ACV PLCL**	0
10% ACV PLGA	0	**10% ACV PLCL**	0
20% ACV PLGA	0	**20% ACV PLCL**	0
10μg ACV	5 ± 3	**No Treatment**	281 ± 8